Selective Control of Electrons in Quantum Wires Formed by Highly Uniform Multiatomic Step Arrays on GaAs(331) Substrates

K.-J. Friedland, H.-P. Schönherr, R. Nötzel, and K. H. Ploog
Paul-Drude-Institut für Festkörperelektronik, Hausvogteiplatz 5-7, D-10117 Berlin, Germany
(Received 31 August 1998)

Coherently aligned, multiatomic step arrays on GaAs(331) substrates generate a periodic array of conductive quantum wires in a two-dimensional (2D) electron gas. A small number of wires is selected by superimposing a constriction with independent side-gate control. By tuning the gate-voltage window, wires can be selected one by one. The resulting oscillatory current transmission provides a new functionality by switching between spatially separated electron channels. The wires are coupled by a small number of 2D electrons resulting in orders of magnitude reduced conductance perpendicular to the step edges.

PACS numbers: 73.23.–b, 73.61.Ey

Semiconductor quantum wires (QWRs) with widths ≤ 100 nm have been widely investigated because of their unique electrical and optical properties, which have a profound impact on basic physics as well as device applications [1,2]. Novel *in situ* growth techniques allow for further developments in the fabrication of dense arrays of QWRs and dots with lateral periodicities of several 10 nm [3,4]. One major advantage in implementing these arrays in future device concepts is the increased current for multiple wires acting in parallel and the related averaging over conductance fluctuations due to defects to provide a well defined output signal [5]. In addition, a higher functionality can be achieved by selective electrical access to a distinct single QWR within the array, which allows for adding, subtracting, and coupling of one-dimensional (1D) conducting channels.

Previous approaches for the formation of dense arrays of QWRs rely on the accumulation of monolayer high step and terrace arrays on vicinal substrates [4,6,7]. However, the high density of kinks and the meandering of the step edges, which cannot be avoided for monolayer high steps, are to a large extent transferred to the multiatomic step arrays (MSA) resulting in pronounced fluctuations in the height and a large number of step crossings limiting the effective length of the wires. The conductance along the wire array between two macroscopic contacts thus includes frequent transitions of carriers from wire to wire, which reduces the conductance and increases conductance fluctuations.

We have recently fabricated highly uniform MSA, which are formed along $[1\bar{1}0]$ on high-index GaAs(331) surfaces by atomic-hydrogen-assisted molecular beam epitaxy [8]. The MSA exhibit a lateral periodicity of 250 nm and are straight over distances >10 μm with minimized height fluctuations. This high structural perfection is related to the microscopic surface structure, which is composed of (110) terraces and (111) steps of similar size, resulting in a higher stability against kink formation during step bunching [9]. The step height can be tuned in a wide range up to 13 nm by the substrate temperature while maintaining the lateral periodicity.

We utilize the MSA as a template for the formation of dense arrays of conductive QWRs by transferring the periodic surface corrugation to the interface of Si modulation-doped $GaAs/Al_{0.3}Ga_{0.7}As$ heterostructures. The two-dimensional (2D) electron transport is highly anisotropic indicating a large anisotropy in the potential and charge distribution. In a sample with a 6 nm high MSA having an electron mobility along the step edges of 22 $m^2\,(V\,s)^{-1}$ for an average 2D electron density of 3×10^{15} m^{-2}, the conductivity ratio parallel and perpendicular to the step edges is larger than ten [8]. However, the microscopic picture of the conductance asymmetry is not revealed in such measurements and has been, indeed, controversially discussed for similar systems [4].

In this paper, we address this problem by investigating the conductance in submicrometer wide constrictions, which are defined in corrugated $GaAs/Al_{0.3}Ga_{0.7}As$ (331) modulation-doped heterostructures. Our goal is to achieve selective electrical access to single QWRs within the array and to investigate their coupling to the surrounding 2D reservoir. The constrictions are electrostatically defined by metallic side gates, which are inserted in 40 nm deep trenches fabricated by electron-beam lithography and wet chemical etching. The 2DEG is located 85 nm below the surface with a spacer layer of 22 nm. The electron gas underneath the gates is almost depleted at zero bias. Two constrictions separated by 20 μm are aligned parallel and perpendicular to the step edges within a conventional Hall bar. All measurements are performed by the four-terminal technique with the Ohmic contacts being far from the constriction for full carrier equilibration. The geometrical width of the constrictions W_{li} amounts to 300–500 nm in different samples, thus containing 2–3 straight step bunches. The two side gates are biased separately to independently control the width of the constriction W_{ef} as well as its lateral position inside W_{li}. The geometric length L_{li} of the constrictions (1–2 μm) is much smaller

 0031-9007/99/83(1)/156(4)$15.00

than the average length of the straight steps enabling quasiballistic transport in the parallel configuration. The lateral layout of the structure is schematically shown in the insets of Figs. 1(b) and 1(c).

The conductance parallel to the MSA shows distinct steps, which persist up to 10 K and are reproducible after temperature cycles up to room temperature, thus proving quasiballistic transport [10]. The conductance as a function of the right-side gate voltage U_R is shown in Figs. 1(a) and 1(b) for several left-side gate voltages U_L. The gate lengths L_{li} are 2 and 1.2 μm, respectively. The steps can be clearly distinguished from the weak, superimposed universal conductance fluctuations originating from inhomogeneous impurity distribution [11]. The changes of the steps with U_L, marked by the dashed lines, indicate spatially separated wires, which carry the current independently. This is confirmed by the steplike decrease of the steps with U_L in the gate-voltage region between -0.8 and -0.5 V [cf. Fig. 1(b)], when the right-side wire becomes depleted in the presence of the changing parallel conductance of the left-side wire. Hence, we conclude that the conductance steps arise from the 1D conductance of *several* parallel conducting QWRs. However, the height of some of the conductance steps deviates from integer multiples of the 1D quantized conductance value $2e^2/h$, which will be discussed in more detail below. In contrast to the

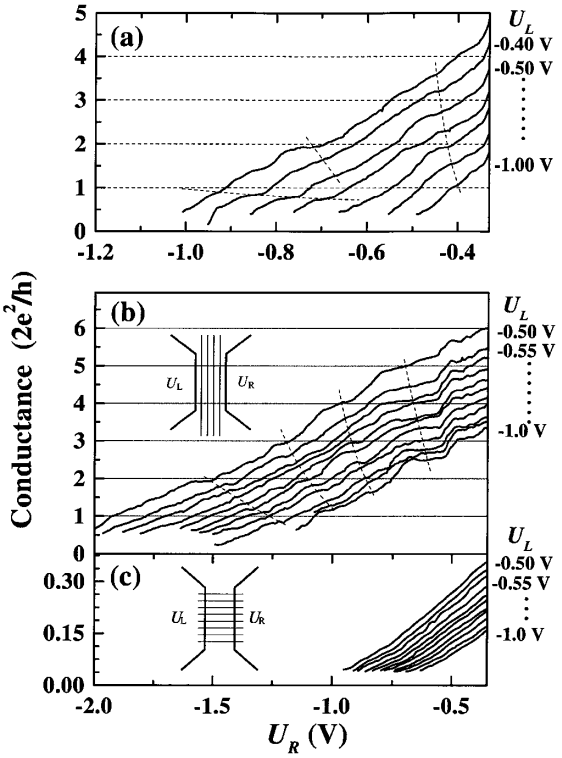

FIG. 1. Wire conductance in a constriction for (a), (b) current parallel and (c) perpendicular to the step edges vs right-side gate voltage U_R recorded at 0.3 K. In (a) $L_{\mathrm{li}} = 2$ μm, while in (b) and (c) $L_{\mathrm{li}} = 1.2$ μm. The parameter is the left-side gate voltage U_L. Note that the conductance scale in (c) is expanded by a factor of 10.

observed quasiballistic transport, the mean free path, calculated to a first approximation from the bulk mobility, is not much larger than the constriction length. However, for the 2D conductivity in large area samples, one has to consider the rigorous carrier scattering from wire to wire due to their finite length, giving a strongly reduced mean free path compared with the ballistic scattering length of carriers in the wires.

The conductance perpendicular to the step edges is much lower than the parallel one as shown in Fig. 1(c). Note the different scales of Figs. 1(a), 1(b), and 1(c). Moreover, the absolute value of the pinch-off voltage U_{po}, at which the width of the depletion layer d_{de} is equal to W_{li}, is significantly smaller for the perpendicular configuration ($U_{\mathrm{po}}^{\perp} \approx -0.8$ V) than for the parallel one ($U_{\mathrm{po}}^{\parallel} \approx -2.1$ V, U_{po} is determined by a linear extrapolation of the gate-voltage dependence of the conductance to zero). This difference is directly related to the periodic modulation of the carrier density in the wire array and indicates the existence of regions of small 2D electron density between the wires, which exhibit a wider depletion zone. Additionally, due to the density modulation, W_{ef} becomes modulated resulting in enhanced side-wall scattering.

Further insight in the 1D conductance of the wires is obtained from Shubnikov–de Haas (SdH) oscillations in magnetotransport experiments. The normalized resistance vs magnetic field B is shown in Fig. 2(a) for different U_L marked by A, B, and C at fixed U_R. The traces exhibit two SdH oscillation periods with the minima denoting the corresponding Landau-level (LL) indices L_1 and L_2. While both periods are present for the conductance plateau A, at the plateau C only one period L_1 remains, indicating the depletion of one of the two QWRs. This confirms the independent conductance along the parallel wires. The dependence of the LL index L_1 on the inverse magnetic field $1/B$ is shown in Fig. 2(c). The clear deviation from the linear dependence for smaller magnetic fields proves 1D confinement of the electron states [12]. Note that the period L_1 is present also in the other traces, and the deviation appears for all values of U_L indicated in Fig. 2(b). The onset of the deviation of the LL index L_1 from a linear dependence corresponds to an electron cyclotron diameter $R_C = \hbar\sqrt{2\pi n_{2\mathrm{DEG}}}/eB$ being comparable to the effective wire width W_{wi}, which is estimated to be 90 ± 20 nm irrespective of the conductance value. Therefore, we interpret W_{wi} as the average width of an individual conducting wire. The carrier density inside the wire $n_{\mathrm{wi}} = (3.5\text{–}5) \times 10^{15}$ m^{-2} is estimated from the linear part. This estimate is not very accurate due to the rather small number of LL indices. However, n_{wi} is clearly larger than the average large-area 2D electron density in agreement with the lateral density modulation across the steps. The number of conducting 1D channels N in this wire is at least equal to or larger than the largest observed LL index of 5 in the SdH experiment, which coincides with N calculated from the wire width according to $N = \mathrm{int}(kW_{\mathrm{el}}/\pi)$

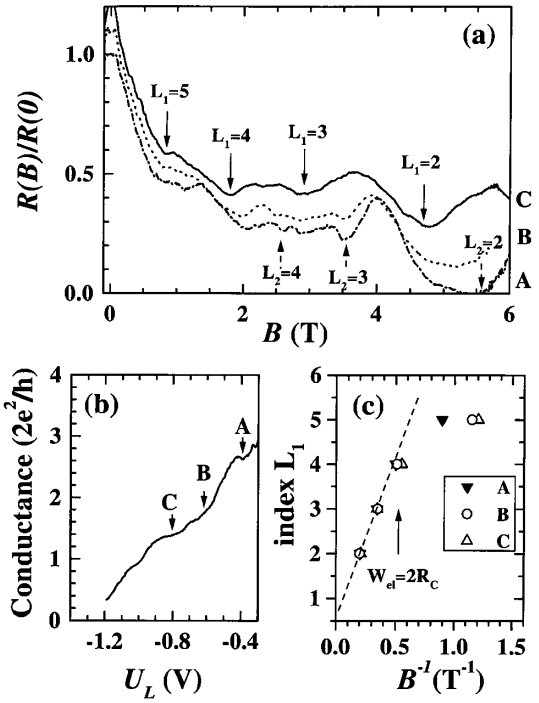

FIG. 2. (a) Normalized resistance vs magnetic field recorded at 0.3 K for three different left-side gate voltages U_L. The curves are shifted by 0.1 with respect to each other. (b) Conductance in a constriction for the current parallel to the step array vs U_L for the right-side gate voltage $U_R = -0.5$ V recorded at 0.3 K. The voltages A, B, and C correspond to the values of U_L for the curves shown in (a). (c) Landau-level (LL) index vs inverse magnetic field for the different curves in (a).

($k^2 = 2\pi n_{\mathrm{wi}}$) giving $N = 4$–5. This corresponds to a confinement energy of about 5 meV. The corresponding measured conductance of 1–2 in units of $2e^2/h$ provides an estimate of the ensemble averaged transmission probability $T = 0.25$–0.5 as defined from the generalized equation $G/(2e^2/h) = N \times T$. This value does not change with the constriction length up to $L_{\mathrm{li}} = 2\ \mu$m. It is thus attributed to backscattering of electrons in a QWR, whose length eventually exceeds L_{li}. This larger guiding length results from imperfect coupling of the corresponding wire to the outer reservoir due to the presence of the interface corrugation over the whole sample area. The transition from the wire to the reservoir can be characterized by the length $l_{2\mathrm{D}}$, over which the 1D electrons are scattered into the 2D states. If $l_{2\mathrm{D}}$ exceeds the backscattering length l_b for the electrons in the QWR, the guiding length of the electrons increases to a length larger than L_{li}, and the transmission will be reduced as $T = 2/(1 + \sqrt{1 + 2l_{2\mathrm{D}}/l_b})$, according to a simple rate equation analysis [13]. For our system, we estimate the ratio $l_{2\mathrm{D}}/l_b$ to be $\approx$5, which characterizes the coupling of a single QWR to the imperfect reservoir. This value reveals a rather weak coupling between spatially separated wires most probably via scattering into the 2D states since the 250 nm distance is too large for direct coupling by tunneling. Vice versa, the weak coupling allows for the independent conductance in spatially separated wires over length scales smaller than $l_{2\mathrm{D}}$, however, producing a transmission probability $T < 1$.

In order to sequentially extract the conductance of spatially separated wires, we study the lateral distribution of the conductance inside the constriction. In Fig. 3 the conductance is shown as a function of $U_P = U_R - U_L$, which determines the lateral position of the effective width inside the constriction. The parameter $\Delta U_W = U_R + U_L - U_{\mathrm{po}}^{\parallel}$ defines a gate-voltage window, i.e., the effective width. In order to eliminate the parallel conductance of the 2D electrons, which affects the traces at larger ΔU_W, we subtract the constant conductance in the perpendicular configuration according to Fig. 1(b) for the same gate-voltage window. At $\Delta U_W < 0.2$ V, two distinct maxima with $G/(2e^2/h) \approx 0.5$ are observed due to the conductance along two separated wires. Upon widening ΔU_W, the conductance trace flattens and subsequently develops a nearly twice as large single maximum at the center position. This behavior can be understood by a self-consistent calculation of the potential and charge distribution of a modulation-doped quantum well used as a model system shown in Fig. 4(a) [14]. Here, we apply the analogous gate effect on the depletion length d_{de} in a coplanar capacitor with that in a sandwich capacitor [15]. In a 2DEG with density $n_{2\mathrm{D}}$ and side-gate depletion voltage U_{de}, $d_{\mathrm{de}} \propto U_{\mathrm{de}}/n_{2\mathrm{D}}$. In contrast, in a doped quantum well with 3D density $n_{3\mathrm{D}}$ and surface depletion charge q_{de}, $d_{\mathrm{de}} \propto q_{\mathrm{de}}/n_{3\mathrm{D}}$. Therefore, if we rescale the depletion voltage by an equivalent depletion charge $q_{\mathrm{de}} = 8\varepsilon n_{3\mathrm{D}}/n_{2\mathrm{D}}U_{\mathrm{de}}$, this calculation provides an estimate of the charge distribution in our system. For the ratio $n_{2\mathrm{D}}/n_{3\mathrm{D}}$ we choose 10 nm, which is close to the Bohr radius of the electrons. Additionally, this

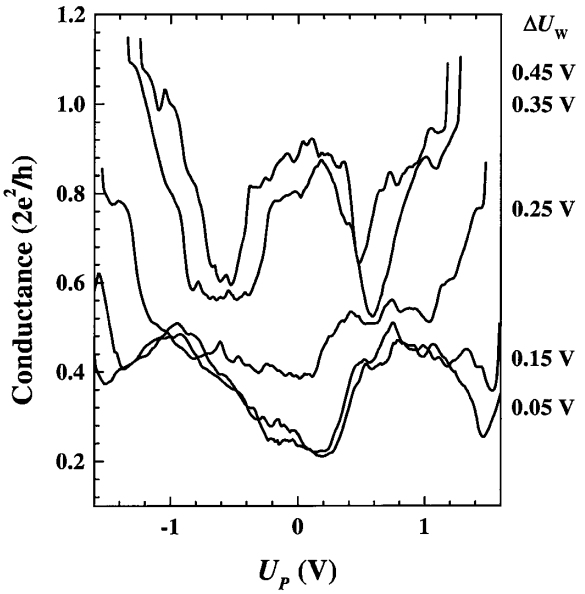

FIG. 3. Conductance in a constriction with current parallel to the step edges vs $U_P = U_R - U_L$ recorded at 0.3 K for different values of the gate voltage window $\Delta U_W = U_R + U_L - U_{\mathrm{po}}^{\parallel}$.

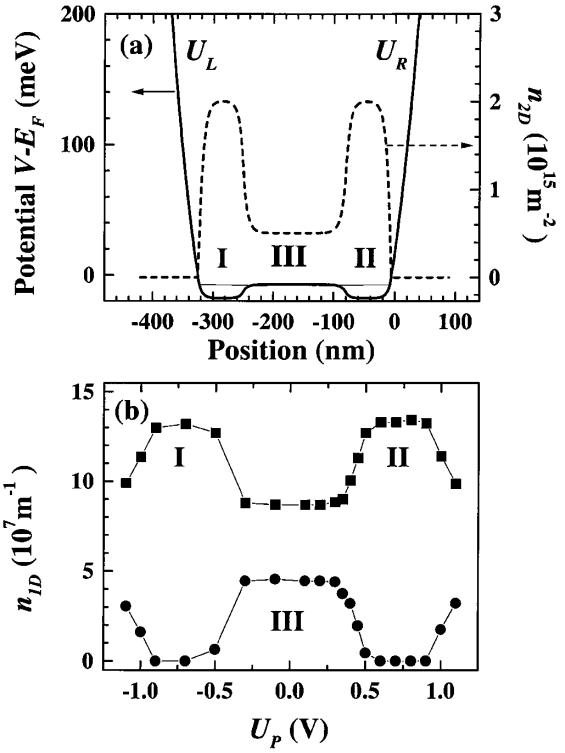

FIG. 4. (a) Calculated lateral potential and 2D carrier distribution in a constriction. U_L and U_R denote the left-side and right-side gate voltages, respectively. The labels I, II, and III indicate the different sublevels described in the text. (b) Calculated 1D carrier density vs U_P for the sublevels I and II (upper curve) and the sublevel III (lower curve) in (a) for a gate voltage window $\Delta U_W = 0.1$ V. The solid line connecting the data points is a guide to the eye.

one-dimensional calculation accounts only for the charge distribution in long wires far away from the contact region to the 2DEG. The doped regions I and II are 70 nm wide with $n_{2D} = 2.0 \times 10^{15}$ m^{-2}. In region III, the doping level is assumed to be 5 times smaller corresponding to the expected carrier profile across the MSA. The corresponding 1D carrier densities for the sublevels I and II (upper curve) and the sublevel III (lower curve) are shown in Fig. 4(b) as a function of U_P for a gate-voltage window $\Delta U_W = 0.1$ V. The three regions correspond to two 1D conducting wires I and II, which are spatially separated by region III. For a small value of ΔU_W, the two conductance maxima in Fig. 3 are due to the two spatially separated 1D wires I and II probed sequentially. The conductance at the center position with $G/(2e^2/h) < 1$ in Fig. 3 arises from the background doping between the wires in region III. For a gate-voltage window centered near one of the edges (region I or II), only one of the two spatially separated wires is conducting, resulting again in a conductance value of approximately 0.5–1. Therefore, at the two conductance maxima in Fig. 3, a single wire is selected from the step array. By simply changing the side-gate voltages, it is thus possible to switch between neighboring wires and, upon widening or closing the gate voltage window, to add or subtract the conductance from spatially separated wires one by one.

In conclusion, the low temperature electron transport in modulation-doped heterostructures grown on highly uniform, multiatomic step arrays on GaAs(331) is governed by coupled one-dimensional wires along the step arrays. Using a narrow constriction with independent side-gate control, we are able to select a single QWR along the step edges. In the present system, the long QWRs are electrically coupled to the reservoir by scattering via a small number of 2D electrons between the wires. These background 2D electrons give rise to orders of magnitude smaller conductance through the constriction aligned perpendicular to the step edges. This system allows for the realization of device concepts based on adding, subtracting, and coupling of neighboring conducting channels.

The authors thank Y. Takagaki and H. T. Grahn for valuable discussions, as well as A. Riedel and I. Poppe for assistance with the sample preparation. Part of this work was supported by the Bundesministerium für Bildung, Wissenschaft, Forschung und Technologie, and NEDO NTDP-98 project.

[1] H. Sakaki, Jpn. J. Appl. Phys. **19**, L735 (1980).
[2] C. W. J. Beenacker and H. v. Houten, *Solid State Physics*, edited by H. Ehrenreich and D. Turnbull (Academic Press, New York, 1991), Vol. 44.
[3] R. Nötzel, D. Eissler, M. Hohenstein, and K. Ploog, J. Appl. Phys. **37**, 431 (1993).
[4] Y. Nakamura, S. Koshiba, and H. Sakaki, Appl. Phys. Lett. **69**, 4093 (1996).
[5] F. Brincop, W. Hansen, J. P. Kotthaus, and K. Ploog, Phys. Rev. B **37**, 6547 (1988).
[6] H. Higashiwaki, M. Yamamoto, T. Higuchi, S. Shimomura, A. Adachi, Y. Okamoto, N. Sano, and S. Hiyamizu, Jpn. J. Appl. Phys. **35**, 606 (1995).
[7] J.-S. Lee, H. Isshiki, T. Sugano, and Y. Aoyagi, J. Cryst. Growth **173**, 27 (1997).
[8] H.-P. Schönherr, J. Fricke, Z. C. Niu, K.-J. Friedland, R. Nötzel, and K. H. Ploog, Appl. Phys. Lett. **72**, 566 (1998).
[9] R. Nötzel, L. Däweritz, and K. Ploog, Phys. Rev. B **46**, 4736 (1992).
[10] S. Tarucha, T. Saku, Y. Tokura, and Y. Hirayama, Phys. Rev. B **47**, 4064 (1993).
[11] P. A. Lee, A. D. Stone, and H. Fukuyama, Phys. Rev. B **35**, 1039 (1987).
[12] K. F. Berggren, T. J. Thornton, P. I. Newson, and M. Pepper, Phys. Rev. Lett. **57**, 1769 (1986).
[13] Y. Tokura and Y. Takagaki (private communication).
[14] K.-J. Friedland and R. Zimmermann, ZIE Report No. 89-3, 65 (1989).
[15] C. Wiemann, M. Versen, and A. Wieck, J. Vac. Sci. Technol. B **16**, 42 567 (1998).